Enhanced Adhesion by Gecko-Inspired Hierarchical Fibrillar Adhesives

Michael P. Murphy,* Seok Kim, and Metin Sitti*

Department of Mechanical Engineering, Carnegie Mellon University, Pittsburgh, Pennsylvania 15213-3890

ABSTRACT The complex structures that allow geckos to repeatably adhere to surfaces consist of multilevel branching fibers with specialized tips. We present a novel technique for fabricating similar multilevel structures from polymer materials and demonstrate the fabrication of arrays of two- and three-level structures, wherein each level terminates in flat mushroom-type tips. Adhesion experiments are conducted on two-level fiber arrays on a 12-mm-diameter glass hemisphere, which exhibit both increased adhesion and interface toughness over one-level fiber samples and unstructured control samples. These adhesion enhancements are the result of increased surface conformation as well as increased extension during detachment.

KEYWORDS: adhesion • bioinspired • dry adhesive • gecko • hierarchy

INTRODUCTION

Adaptation to uneven and rough surfaces is a major feature of biological fibrillar adhesives found in geckos, which exploit intermolecular surface forces such as van der Waals interaction forces to climb (1). Most surfaces are not perfectly smooth; therefore, the gecko has evolved the ability to adhere to surfaces with varying roughnesses. The advantage of these fibrillar adhesives over flat unstructured adhesives for roughness adaptation is that the fibers deform independently, allowing each fiber tip to access deeper recessions to make contact with the surface. Even with the reduced total area due to the spaces between the fibers, the actual contact area can be far greater than that of a flat adhesive in contact with a rough surface because of the multitude of individual contact points (2). When a flat adhesive contacts a rough surface, contact is only made at the highest asperities of the surface, and deformation of the bulk layer is relatively small, leading to an overall low real contact area. Because of their structure, fibrillar adhesives have a much lower effective Young's modulus (3) and can deform to conform to surface roughness. In addition, the low effective modulus prevents the material from returning to its original shape from stored elastic energy while attached to a surface, effectively self-peeling from the surface as seen in unstructured polymers. This allows larger surface roughness asperities to be tolerated. Although the contact area at each tip can be small, the summation of the contact areas of all of the fibers in contact can be significant, particularly if the fibers can stretch or deflect and remain in contact for large extensions. These characteristics are amplified in the case of hierarchical multilevel fibrillar structures, where conformation and effective compliance are increased further by secondary levels of deformation.

In nature, the most advanced fibrillar dry adhesives are found in the heaviest animals that utilize them such as the Tokay gecko, which can weigh up to 300 g. In comparison to the insects whose bodies are much lighter and do not require high-performance adhesion, whose feet contain simple microscale pillars with widened tips, larger animals have more complex adhesive pads with many levels of compliance including their toes, foot tissue, lamellae, and fibers. Additionally, these fibers branch from micron-scale-diameter to submicron-diameter tip fibers, with a fiber structure similar to that of a branching tree or a broom. This multilevel hierarchy allows the adhesive pads to conform to surface roughness with various frequency and wavelength scales. The toes and tissue conform to millimeter-scale roughness, while each subsequent level conforms to roughness at its corresponding size scale. Finally, the submicron terminal tip fibers can access the smallest surface valleys. At the end of each of the terminal fibers is a widened spatula tip, which increases the contact area.

Recently, there has been much interest in developing synthetic adhesives using the same principles as the gecko in both wet (4, 5) and dry conditions (5–10). Simple polymer micropillars with wider flat tips (11), as well as arrays of carbon nanotubes (12), have been demonstrated to adhere to smooth flat surfaces with adhesion strengths surpassing the gecko. However, adhesion to surfaces with micron-scale or greater roughness has proven more challenging (13). In addition, removal of particulate contamination has been demonstrated by continued contacts with a surface in both the gecko foot (14) and synthetic structures (15) or by washing (16–18).

To more closely mimic the structure of the gecko's foot hairs, researchers have attempted to model (19, 20) and fabricate (21) hierarchical fibers with multilevel properties. Spring-based models predict that multilevel hierarchical structures should exhibit higher adhesive force and energy than a one-level structure for a given applied load, due to improved adaptation and attachment ability (19). Ge et al.

* E-mail: mikemurphy@cmu.edu (M.P.M.), sitti@cmu.edu (M.S.).
Received for review December 17, 2008 and accepted February 18, 2009
DOI: 10.1021/am8002439

bundled carbon nanotubes into pillars, which deform together while having individually exposed tips and show increased adhesion compared to nonbundled fibers (22). Photolithography has been used to mold cylindrical micropillars on top of base pillars (23); however, the resulting structures exhibit a significant decrease in adhesion. Kustandi et al. demonstrated a fabrication technique using nanomolding in combination with micromolding to create a hierarchical structure with superhydrophobic properties (24). Until now, no increased adhesion from multilevel branching hierarchical structures has been demonstrated. In this work, we describe novel fabrication techniques for creating hierarchical synthetic fibers, which result in hierarchies from the millimeter to micron scale. Samples fabricated with these techniques are presented, and hemispherical indenter tests are used to examine the effect of hierarchy on the adhesion strength and toughness.

MATERIALS AND METHODS

We have developed several methods to fabricate fibrillar structures with multiple levels of hierarchy. These methods span the size scales from millimeter-scale molding to micron-scale structures. The following sections detail the fabrication processes and initial results of these techniques.

Microscale Hierarchy. Previous fabrication methods (23) create multilevel cylindrical fibers but do not offer much control over the shape of the top-level fibers. As observed in natural fibrillar adhesives and demonstrated previously in synthetic adhesives (11, 25, 26), widened flat tips provide a significant increase in adhesion. Therefore, we have developed a hierarchical fabrication process that includes the formation of specialized tip endings.

This process, which is an extension of a previously described dip-transfer process to form flat mushroom-type tips (11, 25, 27), starts with an array of micropillars with widened flat mushroom tips. The widened tips reduce the amount of vacant space between fibers, allowing more tip fibers to be formed. Thin fibers with wider tips are preferred to cylindrical thicker fibers because they reduce the amount of moment at the fiber tips upon tip rotation, increase the amount of distance between fibers to prevent collisions during shear (26), and have increased compliance. The tips of an array of micromolded vertical or angled polymer microfibers are coated with a layer of liquid polymer by contact against a thin reservoir layer on a donor substrate (Figure 1a). After coating, the wetted fiber tips are placed on an etched silicon wafer (Figure 1c). This master template wafer has micron-scale-diameter cylindrical holes with widened tips formed by deep reactive ion etching, utilizing the notching effect. The fabrication details for these silicon-on-oxide negative templates have been detailed previously (10, 28). Capillary forces draw the liquid polymer into the cavities, which are filled beneath the base fibers. The sample is then left to cure at room temperature for 24 h before the mold is removed using XeF_2 dry etching. When etching is complete, the final hierarchical structures remain (Figure 1d).

Samples fabricated with this process can be seen in Figure 2. Uniformity of the terminal fibers remains a challenge that is currently being investigated, in particular, stiffer materials show promise for maintaining high yield in the terminal fibers. In addition, the initial fabrication of hierarchical structures with submicron-diameter terminal fibers confirms that it is possible to scale this fabrication method down to smaller sizes, more closely mimicking the geometry of the gecko's nanoscale terminal branched fibers.

Macroscale Hierarchy. The previously described technique adds tip fibers onto molded base fibers to create a multilayer

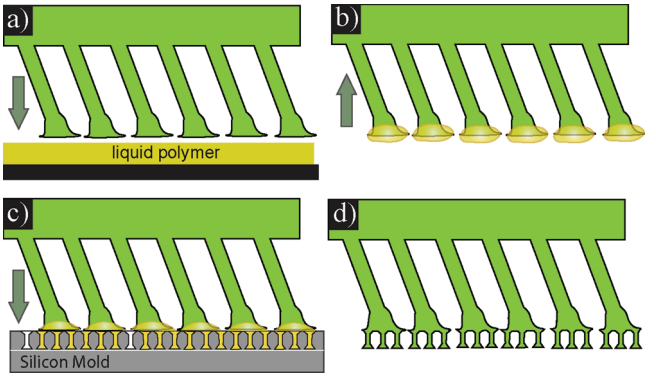

FIGURE 1. Process for the fabrication of hierarchical microfibrillar adhesives with controlled fiber tip shape. (a) Base fibers with mushroom tips are dipped into a donor liquid polyurethane layer. (b) Some of the liquid polymer is retained by the tips. (c) The fiber array is placed onto an etched silicon mold, where the liquid from the tips is drawn into the negative features. d) After the polyurethane has cured, the silicon mold is etched away with a dry etching process.

fibrillar adhesive. Another approach to increasing adhesion of fibrillar structures is to pattern the backing layer *behind* the microscale fibers. Even simple slits in an otherwise unstructured material have been demonstrated to increase the average fracture energy of flat elastomers by an order of magnitude because of inhibited crack propagation (29). This subfiber patterning is seen in the feet of geckos, where the base fibers are attached to thin platelike structures called lamellae. These lamellae increase macroscale compliance and prevent crack propagation. Here, we investigate the use of larger-scale fibers as the patterning of the backing layer. Like the biological lamellae, these fibers act to arrest cracks and increase compliance.

Fabrication of the macroscale base fibers is accomplished by creating a master macrotemplate using a rapid prototyping system (Invision HR, 3D Systems). It is possible to create fibers with diameters as small as 250 μm with this hardware, but the technique is not limited to any particular size scale. Depending on the fabrication method, noncylindrical geometries are possible using this technique. The master template is molded with silicone rubber (HS II, Dow Corning) to create a negative mold. After separation from the master template, the negative mold is used to replicate the base structures from polymers such as polyurethane. Wide flat mushroom tips are added to these base fibers using the dip-transfer method described previously (25). Instead of using a sacrificial silicon mold as in the previous process, a soft silicone elastomer mold is used to create the terminal fibers, and a subsequent dip-transfer tip forming step is performed to add flat mushroom tips to these fibers.

Figure 3 illustrates typical two-level polyurethane fiber structures fabricated using this method. These samples are composed of 50-μm-diameter fibers with 100-μm-diameter mushroom tips atop 400-μm-diameter base fibers with millimeter-scale length and 750-μm- to 1-mm-diameter mushroom tips. The curved base fibers in Figure 3b demonstrate the feasibility of creating complex shapes with this technique. The roughness of the base fibers in the image is due to the relatively low resolution of the rapid prototyped master template; however, this roughness should not affect adhesion because these sections of the fibers do not contact the surface, and may even act to prevent fiber-to-fiber adhesion.

Three-Level Hierarchy. It is possible to combine the macroscale hierarchy fabrication technique with the microscale hierarchy technique to fabricate three-level hierarchical fibers, with each level having widened flat mushroom-shaped tips for

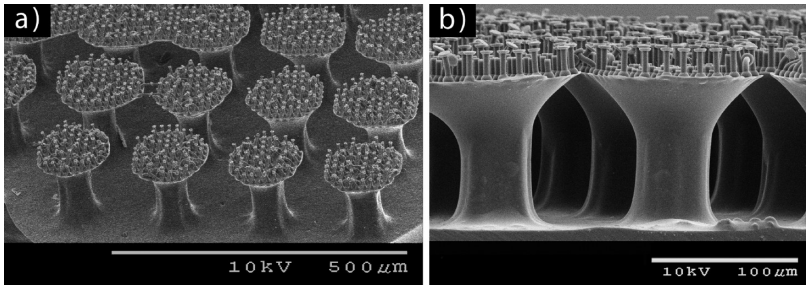

FIGURE 2. Scanning electron micrographs of polyurethane hierarchical fibers with flat mushroom tips. The base fibers have approximately 50-μm-diameter stems with 100-μm-diameter tips, and the tip fibers have 3-μm-diameter stems with 5-μm-diameter tips.

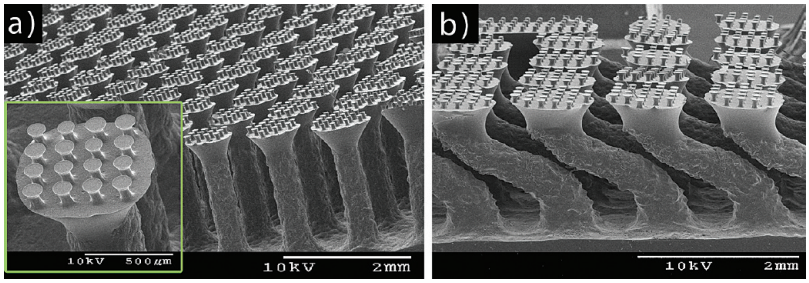

FIGURE 3. Scanning electron micrographs of two-level polyurethane fiber structures: 50-μm-diameter mushroom-tipped fibers atop vertical (a) and curved (b) 400-μm-diameter base fibers with mushroom tips.

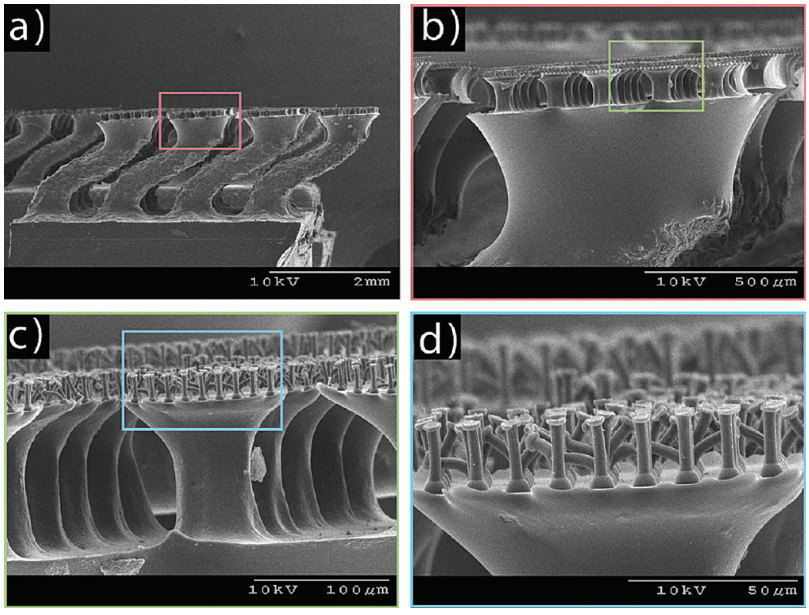

FIGURE 4. Scanning electron micrographs of three-level hierarchical polyurethane fibers: (a) 400-μm-diameter curved base fibers; (b) base fiber tip with midlevel 50-μm-diameter fibers; (c) midlevel fibers in detail; (d) terminal third level fibers at the tip of the midlevel fibers are 3 μm in diameter and 20 μm in height and have 5-μm-diameter flat mushroom tips.

increased area. Combining the processes is relatively straightforward but does require several molding and curing steps to complete.

The initial results of three-level hierarchical fiber fabrication are illustrated in Figure 4. These polyurethane structures exhibit high uniformity, with the exception of the terminal tip fibers. Large stresses from the final release step in fabrication cause some of the microscale tip fibers to collapse as a result of their small diameter and high aspect ratio. Smaller scale fibers composed of stiffer materials are less prone to collapse, so it is likely beneficial to use different materials for each of the hierarchical levels. This can be accomplished using the same fabrication process, simply by molding with stiffer compatible materials for each smaller level of hierarchy. Because of the nonoptimized polymer elastic modulus and fiber release process, the terminal fiber layers in these samples collapse in some regions, which prevented us from characterizing their performance at this time. As a future work, these structures will be fabricated from materials whose stiffness and other physical characteristics are compatible with the fabrication process and compared with one- and two-level fiber samples.

EXPERIMENTS

A polyurethane with an elastic modulus of approximately 3 MPa was used to fabricate four samples, an unstructured control sample, a single-level microfiber sample, a single-level macrofiber sample, and a double-level hierarchical sample, which is a combination of the two single-level fiber structures (Figure 5). Details of the samples can be seen in

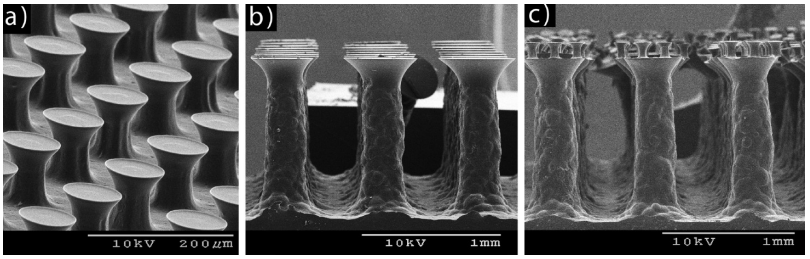

FIGURE 5. Scanning electron micrographs of test samples: (a) single-level micro; (b) single-level macro; (c) double level.

Table 1. Sample Specifications

sample type	base fiber/tip diameter (μm)	base fiber length (mm)	terminal fiber/tip diameter (μm)	terminal fiber length (μm)	total contact area fraction (%)
unstructured					100
single-level micro			50/100	100	29
single-level macro	300/500	1.2			37
double level	300/600	1.2	50/112	100	20

Table 1. These sample geometries were chosen to inspect the effect of combining two levels of fibers into a single structure, versus the adhesion of each fiber level individually. Additionally, the unstructured flat sample is included for comparison. Although the flat mushroom tip shapes appear to be similar to suction cups, previous experiments have shown that vacuum suction does not play a role in adhesion (26).

The unstructured sample was molded against the same substrate so that it has the same surface properties as the fiber samples. The fibers are arranged in square-grid arrays with center-to-center spacing of 160 μm for the microscale fibers and 725 μm for the macroscale fibers. Because the terminal fibers in the single-level microfiber and double-level fiber samples were fabricated from the same mold, they share a similar contact geometry, differing in the contact area fraction, and the structure beneath the terminal fibers. In the single-level micro case, this backing structure is a solid layer of the polyurethane. In the hierarchical sample, this structure is an array of larger base fibers. The base fibers are intended to make the sample effectively more compliant. However, along with the increased compliance, the contact area fraction (total area minus the open space between fibers) is significantly reduced. The total contact area fraction for hierarchical structures is the product of the contact area fraction of each layer. Because the contact area fraction is always less than 100% for fibrillar layers, the total contact area fraction is always decreased by the addition of more levels of hierarchy. For example, the total contact area fraction of the double-level hierarchical samples is the product of the contact area fractions of the terminal and base layers and is therefore the lowest of the four samples. The contact area fraction of the unstructured sample is 100%.

Indentation experiments were performed on the four samples using a 12 mm hemispherical smooth glass indenter. A hemispherical indenter prevents misalignment errors and represents a special case of a rough surface with a well-defined profile and locally smooth surface properties. Because the extension length of the double-level samples is large (millimeter scale), a retraction speed of 200 μm/s was chosen to minimize the duration of the experiments. The approach speed was set to 50 μm/s to avoid significant preload overshoot. Although viscoelastic effects are present because of the relatively high strain rate, which may alter the quantitative characteristics of the adhesion, these experiments are intended to compare the hierarchical structures to single-level fiber and unstructured samples in a relative manner. Five consecutive experiments were performed on the same area of each sample at each specified preload between 2 and 400 mN. The indentation location was changed for each new preload value. The resulting performance curves are plotted together in Figure 6.

Results from the experiments in Figure 6 indicate that the fibrillar samples generally exhibit higher adhesion than the unstructured sample. Particularly at larger preloads, the pull-off force of the fiber samples increase at a faster rate than the increase observed for the unstructured sample. One reason for this increase is that, as the indenter is pressed deeper into contact with the fibers with increasing preloads, the fibers deform and allow neighboring fibers to come into contact with the indenter. This is true for all of the fiber samples, especially the double-level sample, which has

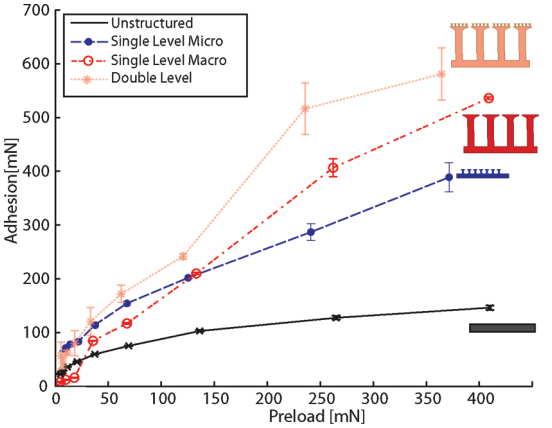

FIGURE 6. Adhesion vs preload data for unstructured, single-level micro, single-level macro, and double-level samples against a 12-mm-diameter glass hemisphere. Error bars represent standard deviations. The double-level fibers generally exhibit the highest adhesion.

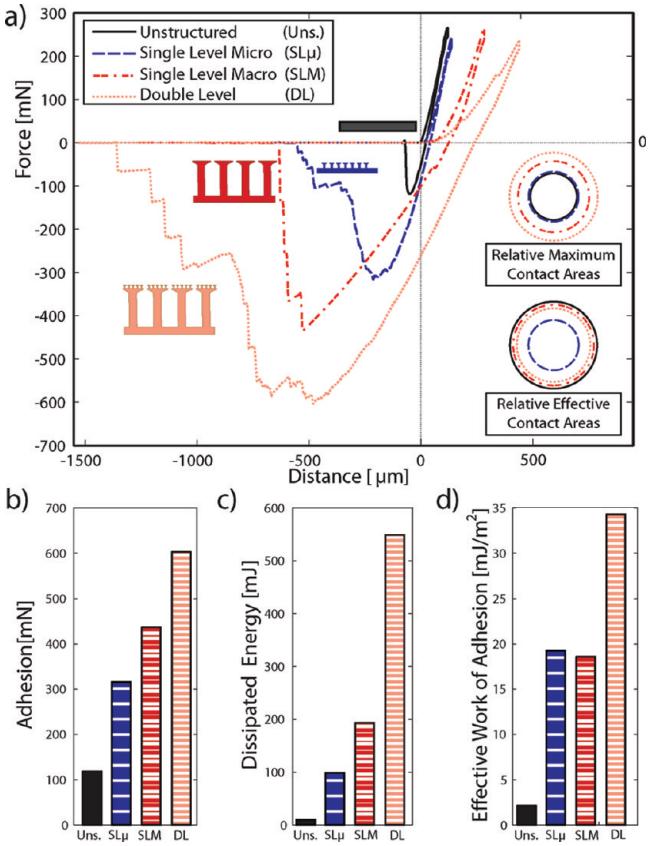

FIGURE 7. (a) Force−distance curves for the samples tested at a preload of 256 mN. (b) Maximum adhesion. (c) Dissipated energy. (d) Effective work of adhesion. The estimated relative contact zone areas and effective contact areas are illustrated as an inset in part a.

highly increased compliance, but not for the relatively stiff unstructured sample. The contact zone of the indenter on the unstructured sample does not increase as much as it does in the case of the fiber samples, so the increase in adhesion with increasing preloads is modest. Although the test equipment did not allow experiments with higher preloads, we predict that adhesion of the single-level fiber samples will saturate at lower preloads than the hierarchical sample because the double-level sample exhibits increased compliance and is taller than the other structures. Therefore, for the double-level sample, the contact area is likely to continue to increase with increased preloads.

Unlike a smooth flat punch indenter, a hemispherical indenter represents a special case of a "rough surface" with a single large smooth asperity. Increased indentation depth with the hemispherical indenter is analogous to increased conformation to asperities and deeper penetration into the valleys of a rough surface. Therefore, these results suggest that the double-level fibers likely exhibit higher adhesion against surfaces with high amplitude (hundreds of micrometers) roughness.

To examine the sample−indenter interaction in more detail, a typical set of force−distance data for the four samples are plotted together in Figure 7. The data are aligned so that the initial contact with the samples occurs where distance = 0. The experimental parameters for these tests were the same as those above, and the preload was set to 256 mN. The adhesions, or pull-off forces, seen as the lowest peaks in the retraction curve, for the samples are compared in Figure 7b. The double-level sample exhibited the highest adhesion, followed by the single-level macrofibers, single-level microfibers, and unstructured samples, respectively.

In these tests, the indentation depths (maximum positive distance) of the indenter for the unstructured sample and single-level sample are similar (120 and 138 μm, respectively). The single-level macro and double-level sample are significantly more compliant, with indentation depths of 283 and 441 μm, respectively, because of their millimeter-scale lengths. Using the indentation depths of from these data, it is possible to estimate the size of the contact zone using the geometrical equations for a spherical cap. The contact zone area a_{cz} is found as

$$a_{cz} = \pi\Delta_p(2R - \Delta_p) \quad (1)$$

where Δ_p is the indentation depth and R is the radius of the hemispherical indenter. The contact zone areas for these tests were found to be 4.5, 5.14, 10.4, and 16.0 mm^2 for the unstructured, single-level micro, single-level macro, and double-level samples, respectively. These estimated contact zones are illustrated as inset illustrations in Figure 7a.

The force−distance data can be used to calculate the energy dissipated during detachment for each of the samples, which, in combination with the contact area, quantifies the toughness of an interface. Dissipated energy is calculated from the area between the approach line and the retraction line for each sample in Figure 7. The high retraction extension observed during separation of the double-level sample requires a higher amount of energy to be expended during detachment. Figure 7c shows the dissipated energy of each sample. Very little energy is required to separate the unstructured sample, while the single-level micro, single-level macro, and double-level samples each require increasingly more energy, with the double-level sample requiring 57 times as much energy as the unstructured sample. Figure 7d shows the effective work of adhesion of each sample, a value calculated by dividing the total dissipated energy by the estimated contact zone area. The fiber samples, even with much larger contact zones and lower contact area fractions, exhibited higher work of adhesion than the unstructured sample. The double-level sample exhibits the highest work of adhesion, 16 times as high as the unstructured sample and nearly twice as high as the single-level samples, despite having the largest contact zone and smallest contact area fraction.

To examine the behavior of a hierarchical sample interacting with an uneven surface, an experiment was run on a separate set if hierarchical fibers while recording a video from a side view of the sample. Frames from the video are shown in Figure 8, illustrating the approach (a), maximum preload condition (b), maximum adhesion (c), last frame before final detachment (d), and fibers returned to their original configuration after separation (e). The maximum

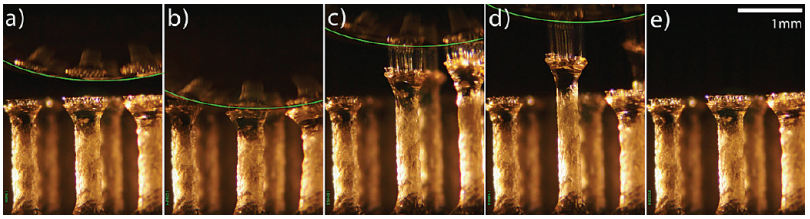

FIGURE 8. Side-view video images from a hierarchical fiber indentation experiment: (a) approach, (b) maximum preload, (c) maximum adhesion, (d) final frame before pull-off, (e) detached fibers returned to their original configuration. The edge of the sphere is outlined for clarity.

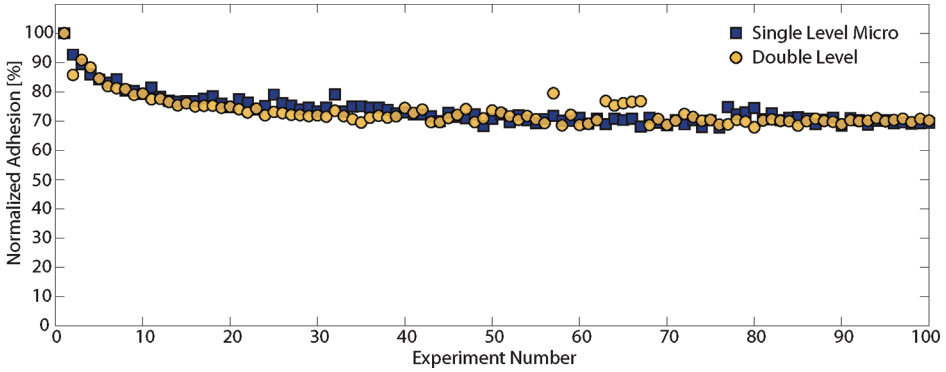

FIGURE 9. Normalized adhesion values for 100 indentation experiments on the same fibers. These data suggest that hierarchical structuring does not affect the repeatability of the adhesives.

preload depth is significantly greater than the length of the terminal fiber layer, which is consistent with data from the previous experiments. During retraction, both the terminal tip and base fibers are observed to stretch as the sample maintains contact with the indenter for large extensions (Figure 8c,d). This video is available in the Supporting Information.

Repeatable adhesion is a highly desirable characteristic of fibrillar adhesives. To examine the adhesive performance during repeated attachment and detachment cycles, sets of indentation experiments were performed on the double-level and single-level micro samples. A total of 100 successive indentation experiments were preformed without moving the samples. The adhesion results from these experiments are illustrated in Figure 9. The preload for the experiments was set to 64 mN, and the results are normalized with respect to the adhesion of the first cycle. Hierarchical structuring of the samples appears to have little effect on repeatability; the adhesion decay of the samples is nearly identical, falling off during the first 40 cycles and leveling off at approximately 70% of the original value for the remainder of the 100 cycles. Previous repeatability tests of the single-level adhesives have shown that, after the initial drop, the adhesion value remains constant for at least 1000 cycles (the maximum number of cycles tested), and the results in Figure 9 suggest that adhesion of the hierarchical samples should exhibit similar long-term repeatability characteristics. Pausing the cyclic experiments and allowing up to 3 h of recovery time did not result in any subsequent increased adhesion, indicating that the adhesion degradation may be irreversible. The exact causes for this degradation are currently being investigated.

SUMMARY

Several techniques for fabricating two-level hierarchical fiber structures on the micro- and macroscales were developed and demonstrated. A three-level hierarchical fiber array with flat mushroom tips was fabricated and presented. Double-level hierarchical structures with mushroom tips were tested with a hemispherical indenter and compared to unstructured and single-level fiber arrays. The hierarchical sample exhibited the highest adhesion to the hemispherical indenter and required significantly more energy to detach than both the single-level macro- and microfiber samples and unstructured control. Adhesion enhancement was found to be due to the increased contact area, which was facilitated by the greatly reduced effective modulus of the sample. These findings are consistent with the previous theoretical analysis of multilevel structures (20). The mechanics of the adhesion and detachment of the hierarchical structures were observed during testing and presented. Both levels of fibers work in concert to stretch and extend to maintain contact with the curved indenter. The results suggest that a hierarchical structure may adhere with higher strength to uneven surfaces with roughness amplitude on the same scale as the length of the base fibers. Double-level structuring was found to have little or no effect on the repeatability of the fibrillar adhesives.

Future work in this area includes testing and characterization of two-level micro hierarchy and three-level hierarchical fibers after suitable fabrication materials and parameters are identified. Characterization of hierarchical structures on real-world surfaces may reveal new insights into the mechanics and applications of multilevel fiber arrays. Combining the three-level fabrication technique with submicron carbon nanotube embedding techniques could yield four-level hierarchical structures with unique properties. Finally,

combining these processes with angled tip processes (26) may facilitate the fabrication of directional hierarchical structures, approaching the performance of the gecko's footpads.

Acknowledgment. The authors acknowledge Burak Aksak for his help in fabrication technique development and assistance in characterization equipment design and construction and Chytra Pawashe for software development.

Supporting Information Available: Video from Figure 8. This material is available free of charge via the Internet at http://pubs.acs.org.

REFERENCES AND NOTES

(1) Autumn, K.; Liang, Y. A.; Hsieh, S. T.; Zesch, W.; Chan, W. P.; Kenny, T. W.; Fearing, R.; Full, R. J. *Nature* **2000**, *405*, 681–685.
(2) Autumn, K.; Peattie, A. M. *Integr. Comp. Biol.* **2002**, *42*, 1081–1090.
(3) Autumn, K.; Majidi, C.; Groff, R. E.; Dittmore, A.; Fearing, R. *J. Exp. Biol.* **2006**, *209*, 3558–3568.
(4) Lee, H.; Dellatore, S. M.; Miller, W. M.; Messersmith, P. B. *Science* **2007**, *318*, 426–430.
(5) Mahdavi, A. *Proc. Natl. Acad. Sci. U.S.A.* **2008**, *105*, 2307–2312.
(6) Sitti, M.; Fearing, R. *J. Adhes. Sci. Technol.* **2003**, *17*, 1055–1074.
(7) Glassmaker, N. J.; Jagota, A.; Hui, C.-Y.; Kim, J. *J. R. Soc., Interface* **2004**, *1*, 23–33.
(8) Greiner, C.; del Campo, A.; Arzt, E. *Langmuir* **2007**, *23*, 3495–3502.
(9) Gorb, S.; Varenberg, M.; Peressadko, A.; Tuma, J. *J. R. Soc., Interface* **2007**, *4*, 271–275.
(10) Kim, S.; Sitti, M. *Appl. Phys. Lett.* **2006**, *89*, 261911.
(11) Campo, A. D.; Greiner, C.; Alvarez, I.; Arzt, E. *Adv. Mater.* **2007**, *19*, 1973–1977.
(12) Qu, L.; Dai, L.; Stone, M.; Xia, Z.; Wang, Z. L. *Science* **2008**, *322*, 238–242.
(13) Aksak, B.; Murphy, M.; Sitti, M. *IEEE Int. Conf. Robot. Autom.* **2008**, 3058–3063.
(14) Hansen, W. R.; Autumn, K. *Proc. Natl. Acad. Sci. U.S.A.* **2005**, *102*, 385–389.
(15) Lee, J.; Fearing, R. S. *Langmuir* **2008**, *24*, 10587–10591.
(16) Bhushan, B.; Koch, K.; Jung, Y. C. *Appl. Phys. Lett.* **2008**, *93*, 093101.
(17) Min, W.-L.; Jiang, B.; Jiang, P. *Adv. Mater.* **2008**, *20*, 1–5.
(18) Sethi, S.; Ge, L.; Ci, L.; Ajayan, P. M.; Dhinojwala, A. *Nano Lett.* **2008**, *8*, 822–825.
(19) Kim, T. W.; Bhushan, B. *Ultramicroscopy* **2007**, *107*, 902–912 (Proceedings of the Eighth International Conference on Scanning Probe Microscopy, Sensors and Nanostructures).
(20) Kim, T. W.; Bhushan, B. *J. Adhes. Sci. Technol.* **2007**, *21*, 1–20.
(21) Jeong, H. E.; Lee, S. H.; Kim, P.; Suh, K. Y. *Colloids Surf. A* **2008**, *313–314*, 359–364.
(22) Ge, L.; Sethi, S.; Ci, L.; Ajayan, P. M.; Dhinojwala, A. *Proc. Natl. Acad. Sci.* **2007**, *104*, 10792–10795.
(23) Greiner, C.; Arzt, E.; del Campo, A. *Adv. Mater.* **2008**, *20*, 1–4.
(24) Kustandi, T. S.; Samper, V. D.; Ng, W. S.; Chong, A. S.; Gao, H. *J. Micromech. Microeng.* **2007**, *17*, N75–N81.
(25) Murphy, M. P.; Aksak, B.; Sitti, M. *J. Adhes. Sci. Technol.* **2007**, *21*, 1281–1296.
(26) Murphy, M. P.; Aksak, B.; Sitti, M. *Small* **2009**, *5*, 170–175.
(27) del Campo, A.; Greiner, C.; Arzt, E. *Langmuir* **2007**, *23*, 10235–10243.
(28) Kim, S.; Aksak, B.; Sitti, M. *Appl. Phys. Lett.* **2007**, *91*, 221913–221915.
(29) Chung, J. Y.; Chaudhury, M. K. *J. R. Soc., Interface* **2005**, *2*, 55–61.

AM8002439